ACS OMEGA

Open Access

This article is licensed under CC-BY-NC-ND 4.0

http://pubs.acs.org/journal/acsodf

Article

Exploring the Capabilities of Nanosized Graphene Oxide as a Pesticide Nanosorbent: Simulation Studies

Prin Tadawattana, Kyohei Kawashima, Sirin Sittiwanichai, Jiraroj T-Thienprasert, Toshifumi Mori,* and Prapasiri Pongprayoon*

Cite This: *ACS Omega* 2025, 10, 8951−8959

Read Online

ACCESS | Metrics & More | Article Recommendations | Supporting Information

ABSTRACT: The pesticide contamination in the environment has become a global concern. So far, pesticide adsorption from waste solution is one of the most economic strategies for pesticide removal. Carbon-based nanomaterials were reported to be potential pesticide sorbents. To date, nanosized graphene oxide (GO) has been discovered. Its nanosize, which is comparable to pesticide sizes, is attractive enough to explore its performance to be the pesticide sorbent. Thus, herein, the adsorption mechanisms of a single pesticide on GO were studied by comparing 6-pesticide systems. Three types of common pesticides (cyfluthrin (CFT) (pyrethroid), ivermectin (IVM) (avermectin), and diazinon (DZ) (organophosphate)) were used as pesticide models. All pesticides rapidly adhere to GO at the graphene-like region. The $\pi-\pi$ and $\pi-$alkyl interactions contribute most to pesticide adhesion. The adsorption of CFT and DZ is led by the $\pi-\pi$ stacking, whereas bulky IVM uses the $\pi-$alkyl forces. Having more pesticides results in self-clustering. Pesticides pile up and avoid lying on the oxygenated area. IVM is the most favorable for GO and shows tight self-packing via dispersion force and hydrogen bonding. Overall, this work displays the encouraging ability of nanosized GO to effectively absorb all pesticides which will benefit future applications in pest control.

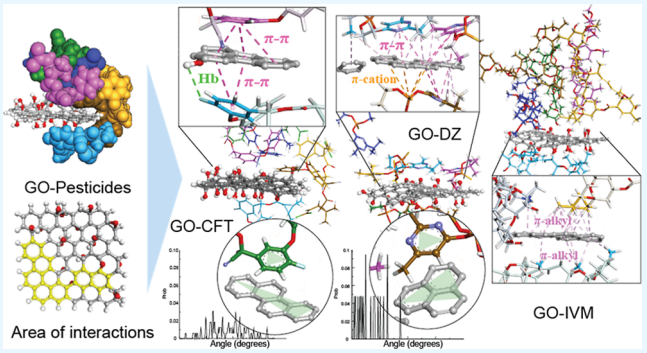

1. INTRODUCTION

Pesticides are substances that are produced by natural or synthetic processes. These are used as one of key ingredients in agricultural developments for shielding agricultural products from pests, weeds, and bacterial and fungal diseases.[1,2] Pesticides are divided into inorganic and organic classes. Previously, diverse inorganic compounds were used to formulate inorganic pesticides including metals (antimony, arsenic, lead, copper, cadmium, and mercury) and metal oxides,[3] but the presence of toxic heavy metals causes high health risks. Organic pesticides were reported to be less toxic to living organisms and more degradable than some inorganic substances.[3] Thus, organic pesticides have largely replaced these inorganic chemicals. Organic pesticides that are currently in use are organophosphates, organochlorines, pyrethroids, and carbamates.[4] Although only small amounts of organic pesticides are required for pest control, such amounts still contaminate the environment. Farmers normally use pesticides to achieve high agricultural productivity, but they are unaware that using excess pesticides leads to more poisonous contamination unfit for consumption. This pesticide contamination can lead to severe conditions including cancers, reproductive harm, genetic changes, neurological toxicity, and endocrine disruption.[4−7] The excess pesticides do not wear off and cause hazard to living entities, especially humans.[4] Owing to the high health risks to humans, many attempts have been made to monitor and detect pesticide content in agricultural products.

Recently, many attempts have been made to not only formulate less toxic and eco-friendly pesticides[8−10] but also collect and quantify pesticides. Biodegradation strategies are also one of eco-friendly techniques.[11] Carbon-based nanomaterials such as graphene oxide (GO) have been reported to be recyclable substances to remove pesticides from wastewater due to its large surface area, high effectiveness in adsorption, and high stability in high pressure and temperature.[9,10,12−15] In addition, GO can be functionalized to target specific contaminants,[16] and its abundance shows the potential to provide cost-effective sorbents.[17] GO is also known to show the excellent photocatalytic properties which can promote the pesticide degradation in water and soil.[18] Therefore, GO was

Received: July 1, 2024
Revised: February 15, 2025
Accepted: February 20, 2025
Published: February 25, 2025

© 2025 The Authors. Published by American Chemical Society

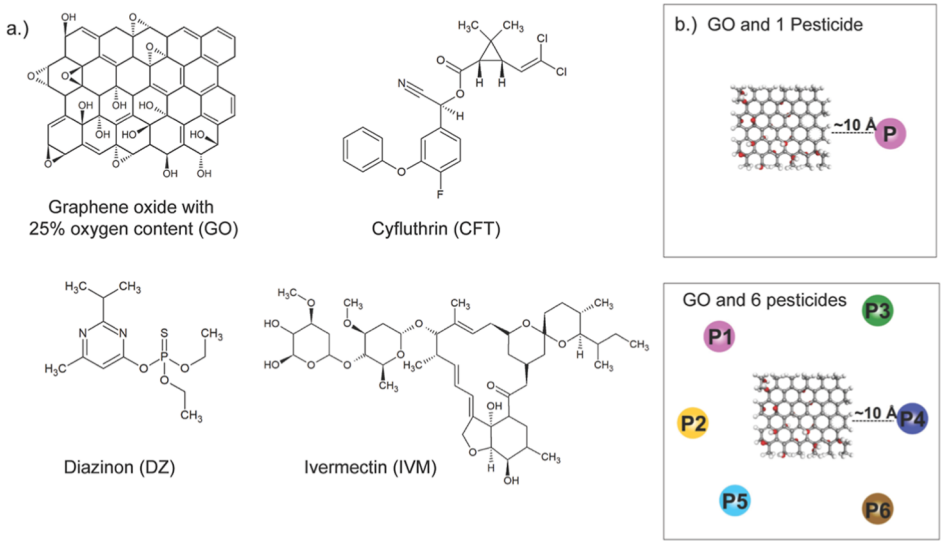

Figure 1. (a) Chemical structures of nanosized graphene oxide with 25% oxygen contents (GO), cyfluthrin (CFT), diazinon (DZ), and ivermectin (IVM). (b) Orientations of pesticides in 1-pesticide and 6-pesticide systems. Pesticides were randomly placed at least 1 nm away from GO. Each bead (P1−P6) represents each pesticide.

reported to be one of tools for environmental remediation technologies.[19] Conventional spectroscopic techniques such as gas chromatography−mass spectrometry (GC−MS) and liquid chromatography−mass spectrometry (LC−MS) are also used to quantify pesticide levels, but such methods require sophisticated instruments and professional skills that are not practical under field conditions. Therefore, many studies have focused on quick and sensitive portable sensors.[20−22] GO was also involved in the pesticide sensor design and development.[23−25] Besides, GO was reported to be used as sorbents because they are recyclable substances and show high effectiveness for pesticide adsorption.[1,26] Earlier, the mechanism of pesticide accumulation on GO was revealed.[26,27] It was reported that the assembly of pesticides onto GO requires $\pi-\pi$ stacking as a major driving force.[9,26,27] In addition, almost all studies focused on microsized graphene and GO as a pesticide sorbent. Recently, nanosized GO has been discovered to display high biocompatibility and low cytotoxicity.[28−30] It was found that the microsized GO was toxic and even caused death to mice, whereas nanosized GO displayed no clear influence on mice.[31] A previous study also reported that a nanosized GO hardly influences human hematopoietic stem cells after 36 h incubation.[32] Importantly, its nanosize which is comparable to pesticide size is attractive enough to explore its performance to adsorb small pesticides for future design of pesticide removal or carrier.

Thus, herein, the capabilities of nanosized GO to adsorb pesticides in solution are investigated. To obtain the adsorption mechanism on the microscopic level, molecular dynamics (MD) simulations were employed. MD simulations have been successfully used to reveal the binding of small molecules on GO including pesticides.[26,27,33,34] Here, we specifically examine the ability of nanosized GO to adhere different types of organic pesticides. Commonly used organic pesticides from different families (cyfluthrin (CFT), ivermectin (IVM), and diazinon (DZ) belonging to pyrethroid, avermectin, and organophosphate families, respectively) are used as pesticide models (Figure 1a). Such pesticides are the main contact pesticides that have a direct effect on human and animal.[35−39] A nanosized GO with 25% oxygen contents was employed as a nanosized GO model (Figure 1a). This GO structure was built based on the Lerf−Klinowski model where the most stable alignment with 2:1 ratio of hydroxyl (−OH) and epoxy (−O−) groups was used.[40] The adsorption mechanism of a single pesticide on GO was studied in comparison to a 6-pesticide system in order to study the effect of pesticide concentration on GO adhesion (Figure 1b). Six pesticides in each system are sufficient to surround a GO sheet in all dimensions to mimic the random pesticide orientations in solution. Since GO has been used as a pesticide carrier,[9,15] the adsorption insights obtained here will be beneficial for designing novel strategies for pesticide removal and carrier.

2. MATERIALS AND METHODS

2.1. Preparation of Nanosized Graphene Oxide and Pesticide Topologies. The structure of nanosized graphene oxide (GO) was constructed by HierGO[41] generated based on the Lerf−Klinowski model. GO with 25% oxygen contents (GO25) was constructed based on a 2:1 ratio of hydroxyl (−OH) and epoxy (−O−) groups, where this ratio was reported to be the most stable alignment.[40] GO has a dimension of 1.5 × 1.3 nm^2 (72 carbon atoms) as seen in Figure 1a. This nanodimension size is comparable to the pesticides studied here. Geometry optimization and normal-mode analysis for GO25 were performed by density functional theory (DFT) at the B3LYP/6-31G(d) level using the Gaussian16 package.[42] Then, the electrostatic potential (ESP) was calculated at the HF/6-31G(d) level. All atomic RESP charges converted from ESP were used to construct topologies using Antechamber from AmberTool20.[43] The three-dimensional structures of pesticides which are cyfluthrin (CFT), diazinon (DZ), and ivermectin (IVM), were built using Discovery Studio 2021[44] and ACPYPE.[45] AMBER14SB was used to construct all of the pesticide topologies.

In this work, six systems were set. Three systems contain one of each pesticide and GO (GO-1CFT, GO-1DZ, and GO-1IVM) and another three systems contain six pesticides with one GO sheet localized at the center of the simulation box (GO-6CFT, GO-1DZ, and GO-6IVM) to mimic high pesticide concentration. Six molecules of pesticides represent

https://doi.org/10.1021/acsomega.4c06036
ACS Omega 2025, 10, 8951−8959

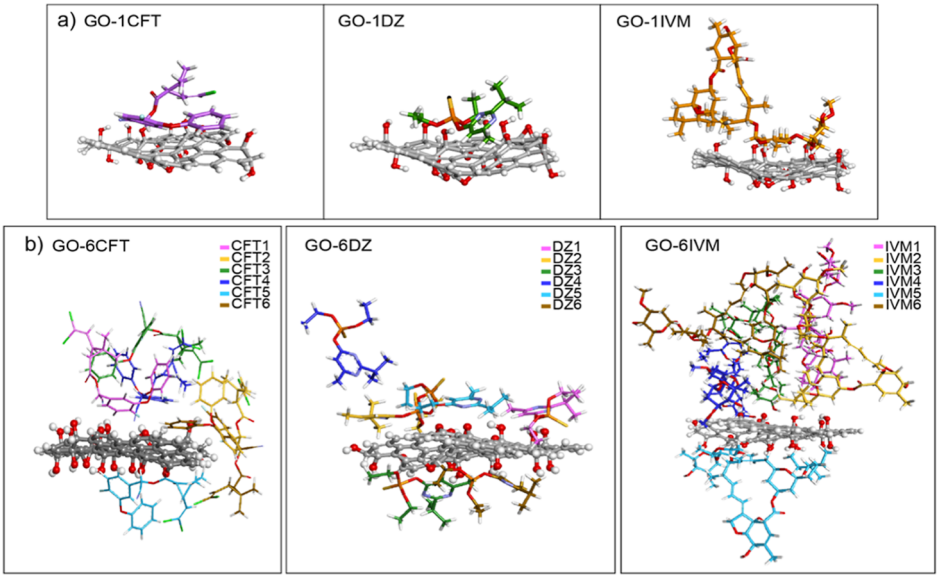

Figure 2. Final snapshots of 1-pesticide systems (GO-1CFT, GO-1DZ, and GO-1IVM) (a) and 6-pesticide systems (GO-6CFT, GO-6DZ, and GO-6IVM) (b).

the presence of pesticides in all directions of GO. In all systems, a pesticide was placed at least 1 nm away from GO in all directions in a simulation box of 6 × 6 × 6 nm^3. The settings can be seen in Figure 1b. Each system was then soaked in TIP3P water molecules. For each system, 1000 steps of energy minimization were run to remove bad contacts with the steepest descent algorithm (the details of the condition used are displayed in the "Simulation Protocols" section). The equilibration run was conducted for 10 ns, followed by the 1 μs production run.

2.2. Simulation Protocols. All molecular dynamics (MD) simulations were performed using the GROMACS2022.7 software package.[46] The electrostatics were treated with Particle mesh Ewald (PME)[47] at 1 nm radius cutoff, a Fourier spacing of 0.12 nm, and fourth-order spline interpolation. The LINCS method[48] was applied to constrain bond lengths within each system. Periodic boundary conditions were applied in all directions. All simulations were performed under constant particle number, pressure, and temperature (NPT) conditions. The Berendsen thermostat[49] was used to maintain the temperature at 300 K with a coupling constant τ_t = 0.1 ps. The pressure was coupled using the Parrinello−Rahman algorithm at 1 bar with a coupling constant of τ_p = 1 ps. The time step for integration was set to 2 fs, and coordinates were saved every 2 ps.

All graphical images were made by Discovery Studio 2021[44] and visual molecular dynamics (VMD).[50] The hydrogen bond counts were operated based on the hydrogen-donor−acceptor cutoff angle and radius of 30° and 0.35 nm, respectively. The binding energies of GO pesticides and self-interaction energies of pesticides were calculated using the Poisson−Boltzmann solver (MM/PBSA) using "gmx mmpbsa" option in GROMACS.[51]

3. RESULTS AND DISCUSSION

Figure 2 shows the final structures after 1 μs simulations for all systems. It is clear that the pesticide adsorption onto nanosized GO is spontaneous in all cases. All pesticides were fully absorbed onto a GO surface (Figure 2). Among the three, IVM and DZ are the bulkiest and smallest molecules, respectively. Thus, a bulky IVM in GO-1IVM is partly exposed to the aqueous solution, whereas GO-1CFT and GO-1DZ seem to align the whole structure on a GO surface (Figure 2a). More detailed analyses will be discussed later in the text. When more pesticide molecules are added, they can fully physisorb on GO where GO-6IVM produces the largest cluster due to its large size (Figure 2b). Most previous theoretical studies explored the adsorption of one pesticide on microsized graphene oxide where such large surface area results in the "laying-flat" conformation of the pesticide.[27] However, this lying-flat conformation becomes the key bottleneck for effective pesticide desorption. Due to the smaller GO structure in the current study, no "laying-flat" conformation is captured in all simulations. This will allow some pesticides to desorb and be detected by probes. Moreover, in 6-pesticide systems, all pesticides can aggregate onto GO and self-assemble at the same time (Figure 2). GO and all pesticides appear to form a stable nanocomposite throughout the course of the simulations. Seemingly, this finding suggests that nanosized GO can act as a good pesticide nanocarrier.

To understand the adsorption mechanism, the number of contacts and hydrogen bonds between GO and pesticides is computed in Table 1. In 1-pesticide systems, the larger IVM molecule shows more GO−pesticide contacts (∼103 contacts) than DZ and CFT (∼44 contacts for CFT and ∼57 contacts for DZ). This implies the tight binding of IVM. Furthermore, bulky IVM seems to be more water-accessible (∼11 hydrogen bonds with water) than DZ and CFT (∼2 hydrogen bonds with water). Nonetheless, each type of pesticides forms only ∼1 hydrogen bond with GO. This indicates the minute role of electrostatic interactions on pesticide adsorption. When increasing the pesticide concentration (6-pesticide systems), each pesticide appears to severely lose its contacts to GO due to self-aggregation (Table 1). Compared to the 1-pesticide system, almost half of the GO−pesticide contacts in all systems are lost during the aggregation, but such loss is compensated by the self-assembly (Table 1). Nonetheless, all pesticides still maintain a hydrogen bond with the GO (Table 1). CFT and IVM lose ∼20−30% of water contacts during the aggregation

https://doi.org/10.1021/acsomega.4c06036
ACS Omega 2025, 10, 8951−8959

Table 1. Number of Contacts and Hydrogen Bonds between Individual Pesticide (Cyfluthrin (CFT), Diazinon (DZ), and Ivermectin (IVM)) with Each Component (GO, Water, and Pesticide) in the Systems[a]

system	pair	no. of contacts	no. of hydrogen bond
GO-1CFT	GO−CFT	44.13 ± 16.00	1.13 ± 0.23
	GO−water	600.82 ± 43.65	26.66 ± 2.57
	CFT−water	150.88 ± 33.59	2.19 ± 1.07
GO-1DZ	GO−DZ	57.82 ± 18.10	1.04 ± 0.48
	GO−water	610.78 ± 41.99	26.35 ± 2.58
	DZ−water	161.67 ± 30.58	1.89 ± 0.97
GO-1IVM	GO−IVM	103.98 ± 18.30	1.00 ± 0.45
	GO−water	571.51 ± 37.82	25.79 ± 2.55
	IVM-water	512.69 ± 47.90	11.11 ± 1.85
GO-6CFT	GO−CFT	26.48 ± 3.17	1.03 ± 0.03
	CFT−CFT	16.81 ± 0.81	
	GO−water	481.84 ± 50.95	24.13 ± 2.70
	CFT−water	103.54 ± 33.85	1.83 ± 0.97
GO-6DZ	GO−DZ	36.39 ± 3.63	1.07 ± 0.06
	DZ−DZ	21.06 ± 1.73	
	GO−water	477.86 ± 47.71	23.18 ± 2.65
	DZ−water	160.96 ± 43.12	2.17 ± 1.17
GO-6IVM	GO−IVM	52.53 ± 29.09	1.19 ± 0.67
	IVM−IVM	38.11 ± 32.66	1.00 ± 0.45
	GO−water	409.90 ± 47.48	21.07 ± 2.62
	IVM−water	416.48 ± 60.25	6.32 ± 1.32

[a]The contacts are counted when all pairs between two chosen components are in the cut-off distance of 0.35 nm.

in GO_6CFT and GO_6IVM, whereas enhancing DZ concentration does not disrupt DZ−water contacts. DZ in both GO_1DZ and GO_6DZ remains surrounded by water via ∼160 contacts (Table 1). Also, it is expected that GO becomes less water-exposed in 6-pesticide cases (∼100 GO−water contacts are lost) (Table 1).

To further investigate how each pesticide interacts with GO, the number of contacts between GO and main functional groups of each pesticide (cyclopropane-carboxylate ester for CFT, organophosphorus for DZ, lactone, and a group of disaccharides, benzofuran, and spiroketal for IVM) is computed in Figure 3. Compared to the total contacts in Table 1, the number of DZ−GO and IVM−GO contacts (parent group−GO contacts, where parent groups are phosphate ester of DZ and lactone of IVM (red and cyan labels in Figure 3b)) in Figure 3a is smaller, indicating that both do not require their parent groups to interact with GO (Figure 3). Rather, both DZ and IVM employ the rest of the structure to adhere to GO (Figure 3). For CFT, its carboxylate ester appears to play a role in the adsorption where 30% of the total CFT−GO contacts are obtained from its functional group (cyclopropane-carboxylate ester; Table 1 and Figure 3a). Moreover, the hydrogen bond found in Figure 3a for DZ and CFT demonstrates that the total number of GO−pesticide hydrogen bonds found in Table 1 is rooted from a parent group of DZ and CFT. Unlike others, IVM seems to employ the side chain moieties to hydrogen bond to GO (Figure 3). The results obtained demonstrate that each type of pesticide employs nonidentical mechanisms to interact with GO. The hydrophobic interactions were reported to contribute most to GO−pesticide adsorption.[27,33,52−54] The pesticides studied here are consistent with this trend since only one hydrogen bond is captured (Table 1 and Figure 3a) while a large number of contacts are found. This highlights the role of hydrophobic interaction for adhesion. In addition, we further decompose the adsorption mechanism of each type of existing pesticides in detail later in the text.

To better understand the effect of chemical properties of each pesticide on the adsorption ability, the binding energies between each component (GO−pesticide and pesticide−pesticide) are computed in Table 2. The high Vdw energies observed in all cases confirm that the hydrophobic interactions contribute most to pesticide adhesion. These binding energies

a)

System	Pair	No. of contacts	No. of hydrogen bond
GO-1CFT	GO-CFT	14.96 ± 10.04	1.20 ± 0.20
GO-1DZ	GO-DZ	6.42 ± 4.28	1.04 ± 0.47
GO-1IVM	GO-IVM	91.42 ± 15.67	1.00 ± 0.45
	GO-IVM	10.59 ± 6.08	-
GO-6CFT	GO-CFT	12.84 ± 8.80	1.01 ± 0.26
GO-6DZ	GO-DZ	5.69 ± 3.93	1.05 ± 0.33
GO-6IVM	GO-IVM	42.94 ± 15.42	1.18 ± 0.52
	GO-IVM	14.21 ± 7.89	-

b)

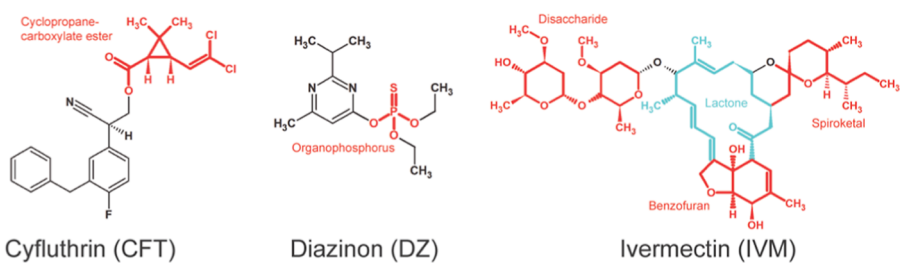

Figure 3. (a) Number of pesticide−GO contacts and hydrogen bonds in all systems. Only the contacts and hydrogen bonds between key chemical families of each pesticide and GO are computed. The chemical families of each pesticide are shown in red (cyclopropane-carboxylate ester for CFT, organophosphorus for DZ, a group of disaccharides, benzofuran, and spiroketal for IVM) and cyan (lactone) in (b).

https://doi.org/10.1021/acsomega.4c06036
ACS Omega 2025, 10, 8951−8959

Table 2. Average Binding Energies (kJ/mol) between Each Component (GO and Pesticide) with Standard Deviation in All Systems Using MMPBSA[a]

system		VdW	elec	total
GO-1CFT	GO−CFT	−94.15 ± 30.48	−6.97 ± 10.79	−100.52 ± 34.28
GO-1DZ	GO−DZ	−104.44 ± 23.88	−12.10 ± 5.39	−116.54 ± 31.83
GO-1IVM	GO−IVM	−144.87 ± 16.28	−16.48 ± 8.37	−161.34 ± 18.30
GO-6CFT	GO−CFT	−34.53 ± 37.27	−5.31 ± 10.24	−39.84 ± 43.80
	CFT−CFT	−12.54 ± 16.69	−1.53 ± 3.67	−14.07 ± 18.97
GO-6DZ	GO−DZ	−48.85 ± 36.28	−8.67 ± 13.62	−57.51 ± 43.69
	DZ−DZ	−6.81 ± 11.93	−1.32 ± 4.11	−8.13 ± 15.02
GO-6IVM	GO−IVM	−62.48 ± 23.76	−14.52 ± 10.77	−77.00 ± 30.09
	IVM−IVM	−29.41 ± 15.30	−1.73 ± 3.51	−31.15 ± 17.19

[a]VdW and Elec denote the van der Waals and electrostatic energies, respectively, and Total is the sum of VdW and Elec terms.

Table 3. Number of Contacts in 6-Pesticide Systems (GO-6CFT, GO-6DZ, and GO-6IVM)

system		CFT1	CFT2	CFT3	CFT4	CFT5	CFT6	water
GO-6CFT	**GO**	24.23 ± 17.36	27.13 ± 18.86	32.56 ± 20.89	24.46 ± 17.82	25.79 ± 17.80	24.68 ± 18.99	481.84 ± 50.95
	CFT1		15.95 ± 12.41	17.51 ± 13.76	17.44 ± 13.87	16.61 ± 12.77	16.24 ± 13.02	107.89 ± 34.61
	CFT2			17.24 ± 13.95	15.34 ± 12.37	16.44 ± 13.10	16.72 ± 13.47	104.41 ± 34.06
	CFT3				16.82 ± 13.30	16.89 ± 12.86	18.93 ± 14.87	95.36 ± 33.57
	CFT4					16.47 ± 13.32	16.56 ± 12.95	107.35 ± 30.88
	CFT5						16.96 ± 13.39	105.75 ± 34.01
	CFT6							100.48 ± 36.03
		DZ1	**DZ2**	**DZ3**	**DZ4**	**DZ5**	**DZ6**	water
GO-6DZ	**GO**	37.80 ± 22.04	33.12 ± 21.18	40.53 ± 24.76	39.30 ± 23.84	36.46 ± 22.49	31.14 ± 19.74	477.86 ± 47.71
	DZ1		20.81 ± 12.18	18.78 ± 10.84	21.93 ± 12.92	23.30 ± 14.58	22.41 ± 14.56	154.73 ± 40.07
	DZ2			19.41 ± 11.52	21.65 ± 12.70	22.71 ± 13.09	19.24 ± 11.74	167.46 ± 43.50
	DZ3				19.16 ± 10.80	21.48 ± 11.85	23.14 ± 13.85	162.88 ± 44.74
	DZ4					20.06 ± 10.80	23.24 ± 14.92	155.66 ± 43.10
	DZ5						18.57 ± 10.91	166.00 ± 46.30
	DZ6							159.06 ± 42.05
		IVM1	**IVM2**	**IVM3**	**IVM4**	**IVM5**	**IVM6**	water
GO-6IVM	**GO**	45.83 ± 21.30	32.94 ± 17.54	22.88 ± 13.66	45.67 ± 17.90	105.20 ± 15.54	62.67 ± 33.09	409.90 ± 47.48
	IVM1		82.26 ± 45.54	63.04 ± 33.99	25.93 ± 15.85	6.94 ± 2.14	18.40 ± 13.30	438.29 ± 53.17
	IVM2			47.83 ± 27.24	49.28 ± 31.14	8.22 ± 3.97	38.72 ± 34.83	426.38 ± 76.11
	IVM3				113.10 ± 23.12	0.00 ± 0.00	23.64 ± 19.98	359.60 ± 56.11
	IVM4					4.69 ± 2.57	69.83 ± 18.59	326.16 ± 69.27
	IVM5						19.81 ± 11.32	498.86 ± 48.45
	IVM6							449.60 ± 58.36

agree well with previous studies.[27,53,55,56] Among all, IVM shows better binding affinity (binding energies of −161.34 kJ/mol in GO_1IVM and −77.00 kJ/mol in GO_6IVM) to GO than to DZ and CFT in all cases. DZ and CFT display a comparable degree of binding affinities in 1-pesticide systems, but DZ in GO-6DZ becomes more preferable for GO than CFT in 6-pesticide systems (GO-6CFT) (Table 2). Seemingly, the binding affinities of all pesticides on GO are severely reduced under a high pesticide concentration (Table 2). A high number of pesticides induce the self-clustering with different degrees of compactness. Bulky IVM molecules form a cluster (IVM−IVM binding energy of −31.15 kJ/mol), while DZs are more dispersed (binding energy of −8.13 kJ/mol) (Table 2). Although the interactions with GO are the main attractive forces to trap all pesticides on a GO surface, the self-clustering interactions also play a role in pesticide adsorption, especially in GO_6CFT and GO_6IVM (Table 2). DZs in GO-6DZ can also self-interact but are less favorable than other pesticides (DZ−DZ binding energy of −8.13 kJ/mol) (Table 2). The standard deviations of the energies are large in the 6-pesticide systems because of the diffusive dynamics of pesticides. In CFT and DZ, all molecules move diffusively toward GO, where all appear to gain a comparable number of GO (∼25−32 contacts for CFT and 31−40 contacts for DZ) and self-contacts (∼15−19 contacts for CFT and ∼19−23 contacts for DZ) (Table 3). Each molecule of CFT and DZ seems to equally contribute to interact with GO. On the contrary, different bound IVM conformations on GO are observed (Table 3). IVM5 is fully adhered on one side of the GO surface at the beginning of a simulation resulting in high GO contacts (∼105 contacts) (Table 3 and Figure 4b). Unlike IVM5, IVM3 is literarily packed at the outermost of the IVM cluster, leading to the least GO contacts (∼22 contacts) (Table 3 and Figure 4c). Bulky IVMs appear to act differently from CFT and DZ. Some IVMs show high self-contacts, while others display high GO contacts (Table 3). This implies different degrees of GO accessibility. The high IVM−IVM contacts reflect not only the favorable self-assembly but also the steric hindrance of its structure that blocks the GO accessibility. The self-clustering of pesticides can also be seen in GO-free systems with similar levels of self-binding energies to GO−pesticide systems (Figure S1 and Table S1 in the

https://doi.org/10.1021/acsomega.4c06036
ACS Omega 2025, 10, 8951−8959

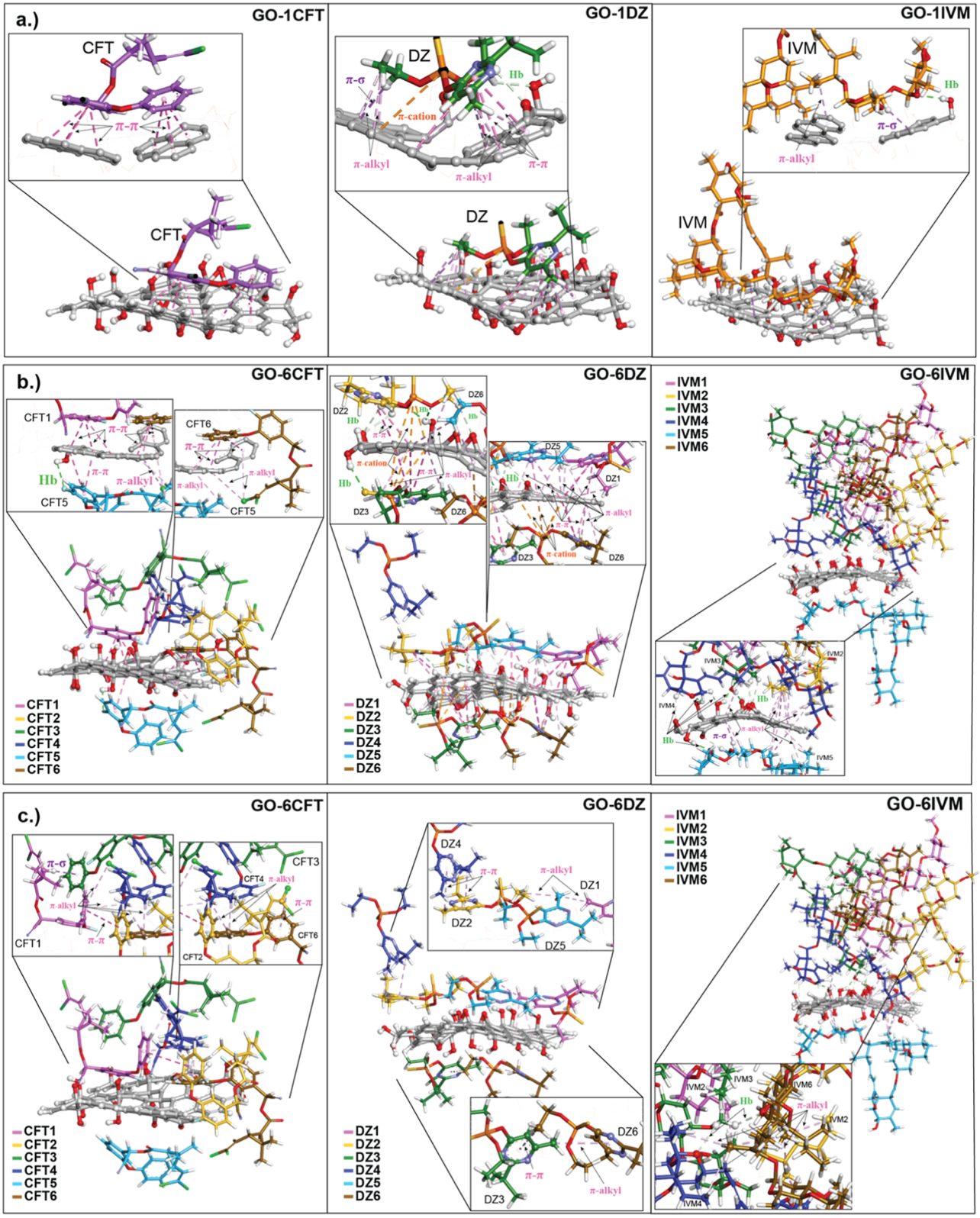

Figure 4. Cartoon representations of 1-pesticide (a) and 6-pesticide (b,c) systems where key interactions are shown as insets.

Supporting Information). However, only loose packing of small CFT and DZ is captured because of the presence of free CFT and DZ in the bulk (Figure S1 in the Supporting Information). Having GO appears to effectively collect all pesticides. This indicates that GO can serve as a promoter for pesticide aggregation.

In previous studies, not only $\pi-\pi$ stacking but also other hydrophobic forces such as alkyl-π interactions were reported to play a role in the GO adsorption.[27,33,52−54] Even though π interactions cannot be directly captured by molecular mechanics, such interactions can be evident from the planar orientations of aromatic moieties toward GO for $\pi-\pi$ stacking

https://doi.org/10.1021/acsomega.4c06036
ACS Omega 2025, 10, 8951−8959

(planar angle ≤20°[54,57]) and constant distance between alkyl chain and GO for π-alkyl interactions. Recent theoretical studies have reported that the π−alkyl dispersion forces can exist within a C−C distance of 0.45 nm.[52,54] In this work, the π−π and π−alkyl dispersion forces are found to play a vital role in the pesticide adsorption. High number of contacts between the graphene-like region and pesticides demonstrate that all pesticides prefer the graphene-like zone to the polar region (Figure S2 and Table S2 in the Supporting Information). For the 1-pesticide system, CFT and DZ are mainly trapped on the GO surface by planar π−π interactions in assistance with one hydrogen bond (Figures 4a and S3 in the Supporting Information). On the other hand, IVM employs only π−alkyl forces and a hydrogen bond for GO binding due to the absence of aromaticity (Figures 4a and S3 in the Supporting Information). In the case of a hydrogen bond, the single adsorbate−GO hydrogen bond obtained in CFT and DZ is formed by their parent groups (carboxylate ester for CFT and organophosphate for DZ), while IVM utilizes nonlactone moieties for hydrogen bonding (Figures 3 and 4). The larger size also allows IVM to form more interactions, resulting in the best binding energy (Figures 3 and 4).

In the case of 6-pesticide systems, the adsorption on GO appears to rely on the "first come first served" basis. A first few molecules start to land on the deoxygenated region and mainly interact with GO via π interactions (π−π stacking for CFT and DZ and π−alkyl interactions for IVM) (Figures 4 and S4 in the Supporting Information). When the graphene-like zone on GO is completely occupied, the other pesticides tend to pile up on top of GO-bound pesticides rather than line up on the oxygenated area (Figures 1, 4c, and S2b in the Supporting Information). This is why the pesticide adhesion on to GO lacks hydrogen bonding (only ∼1 GO−adsorbate hydrogen bond is found for all GO−pesticide systems). The binding energies display IVM as the most favorable species on GO (Table 2) because bulky IVMs are packed upright, allowing the polar moieties to hydrogen bond with adjacent molecules (Figure S5 in the Supporting Information). This self-packing in the assistance of a hydrogen bond allows more favorable IVM−GO clustering. On the contrary, CFT and DZ show no significant self-hydrogen bond, but their self-aggregation on GO is facilitated by π−π and π−alkyl interactions (Figures 4c and S4 in the Supporting Information). This finding can explain why IVM displays better binding energies than the other two (Table 2). The force fields used in this work can capture the key interactions between GO and pesticides as seen in other quantum calculations and MD simulations with other generalized force fields.[26,27,58,59] This indicates the reliability of the force fields used in this work.

4. CONCLUSIONS

Herein, the aggregation mechanisms of commonly used pesticides (CFT, DZ, and IVM) on nanosized GO are investigated for the first time. All pesticides are rapidly and spontaneously adsorbed on GO without desorption throughout the course of all simulations. Overall, nanosized GO exhibits promising potential as a pesticide sorbent. All types of pesticides here prefer a deoxygenated area for adsorption, while they can also hydrogen bond with an oxygenated area. The adsorption affinities of all of the adsorbates here depend on the degree of hydrophobicity. GO with high oxygen contents seems to be inappropriate for effective pesticide adsorption. Among all of these, IVM appears to act as the best adsorbate. Although bulky IVM cannot form any π−π interaction owing to the lack of aromaticity, it can favorably be stabilized on the GO surface by multiple π−alkyl interactions and hydrogen bonds. In addition, IVM are also clustered on GO using both hydrophobic and electrostatic interactions, whereas the self-packing of CFT and DZ employs only π interactions. Thus, more interactions found in the IVM allow tighter binding. Taken together, both favorable GO-binding affinities and self-clustering allow IVM to become the best adsorbate.

The results here suggest that nanosized GO can act as a potential pesticide sorbent. Furthermore, each pesticide displays different degrees of accumulation affinities on GO, suggesting the feasibility of sequential pesticide extraction for further detection. Recently, microsized GO has been studied as a pesticide carrier. Such composite was reported to act as a high-efficiency carrier.[9,10] GO also showed the synergistical effect with pesticides to improve control efficacy and utilization efficiency.[8,60] While this pesticide−GO composite displays the high fungicide and insecticide activities,[9,10,60] microsized GO can be toxic to hosts such as crop or livestock. This is because large-sized GO was reported to be toxic to various species, while cytotoxicity is reduced in nanosized GO.[61,62] Thus, the encouraging ability of nanosized GO to effectively adsorb all pesticides similar to large-sized GO found here suggests the safer application potential in pest control of nanosized GO.

■ ASSOCIATED CONTENT

Supporting Information

The Supporting Information is available free of charge at https://pubs.acs.org/doi/10.1021/acsomega.4c06036.

Final snapshots of GO-free pesticide systems (6CFT, 6DZ, and 6IVM) at 150 ns; chemical structure of GO where the graphene-like region; cartoon representatives of π−π and π−alkyl orientations observed in GO-1CFT, GO-1DZ, and GO-1IVM; cartoon representatives of π−π and π−−alkyl orientations observed in GO-6CFT, GO-6DZ, and GO-6IVM; final snapshots of all 6-pesticide systems; average binding energies (kJ/mol) between pesticides with standard deviation in all systems using MMPBSA; and number of pesticide contacts with graphene-like and oxygenated regions (PDF)

■ AUTHOR INFORMATION

Corresponding Authors

Toshifumi Mori − *Institute for Material Chemistry and Engineering, Kyushu University, Kasuga, Fukuoka 8168580, Japan; Interdisciplinary Graduate School of Engineering Science, Kyushu University, Kasuga, Fukuoka 8168580, Japan;* orcid.org/0000-0003-0188-0794; Phone: +66-2562-5555; Email: toshi_mori@cm.kyushu-u.ac.jp

Prapasiri Pongprayoon − *Department of Chemistry, Faculty of Science, Kasetsart University, Bangkok 10900, Thailand; Center for Advanced Studies in Nanotechnology for Chemical, Food and Agricultural Industries, KU Institute for Advanced Studies, Kasetsart University, Bangkok 10900, Thailand;* orcid.org/0000-0002-1472-8241; Phone: +81-92-583-7800; Email: fsciprpo@ku.ac.th

Authors

Prin Tadawattana − *Department of Chemistry, Faculty of Science, Kasetsart University, Bangkok 10900, Thailand*

https://doi.org/10.1021/acsomega.4c06036
ACS Omega 2025, 10, 8951−8959

Kyohei Kawashima − *Institute for Material Chemistry and Engineering, Kyushu University, Kasuga, Fukuoka 8168580, Japan;* orcid.org/0000-0002-9335-8145
Sirin Sittiwanichai − *Department of Chemistry, Faculty of Science, Kasetsart University, Bangkok 10900, Thailand*
Jiraroj T-Thienprasert − *Department of Physics, Faculty of Science, Kasetsart University, Bangkok 10900, Thailand;* orcid.org/0000-0001-5611-9607

Complete contact information is available at: https://pubs.acs.org/10.1021/acsomega.4c06036

Notes

The authors declare no competing financial interest.

■ ACKNOWLEDGMENTS

We would like to thank Kasetsart University Research and Development Institute (grant no. FF(KU)51.67), Grant-in-Aid for Scientific Research (Grant Nos. 22H02035, 23K23303, and 23KK0254) from JSPS, the Office of the National Economic and Social Development Council, and the Office of the Prime Minister through Kasetsart University under the project entitled "Driving Research and Development of Cutting-edge Innovations for ASEAN's Agricultural Leadership" for financial support. The calculations were carried out at Kasetsart University HPC service center (Nontri AI) and the Research Center for Computational Sciences in Okazaki (Project Nos. 23-IMS-C111 and 24-IMS-C105).

■ REFERENCES

(1) Dasriya, V.; Joshi, R.; Ranveer, S.; Dhundale, V.; Kumar, N.; Raghu, H. V. Rapid detection of pesticide in milk, cereal and cereal based food and fruit juices using paper strip-based sensor. *Sci. Rep.* **2021**, *11* (1), 18855.
(2) Meshram, S.; Bisht, S.; Gogoi, R. Current development, application and constraints of biopesticides in plant disease management. In *Biopesticides*; Elsevier, 2022; pp 207−224.
(3) Hassan, A. S. Inorganic-based pesticides: a review article. *Egypt Sci. J. Pestic* **2019**, *5*, 39−52.
(4) Thorat, T.; Patle, B.; Wakchaure, M.; Parihar, L. Advancements in Techniques Used for Identification of Pesticide Residue on Crops. *Journal of Natural Pesticide Research* **2023**, *4*, 100031.
(5) Damalas, C. A.; Koutroubas, S. D. Farmers' Exposure to Pesticides: Toxicity Types and Ways of Prevention. *Toxics* **2016**, *4* (1), 1.
(6) Park, B. K.; Kwon, S. H.; Yeom, M. S.; Joo, K. S.; Heo, M. J. Detection of pesticide residues and risk assessment from the local fruits and vegetables in Incheon, Korea. *Sci. Rep.* **2022**, *12* (1), 9613.
(7) Mostafalou, S.; Abdollahi, M. Pesticides and human chronic diseases: evidences, mechanisms, and perspectives. *Toxicol. Appl. Pharmacol.* **2013**, *268* (2), 157−177.
(8) Li, X.; Wang, Q.; Wang, X.; Wang, Z. Synergistic Effects of Graphene Oxide and Pesticides on Fall Armyworm, Spodoptera frugiperda. *Nanomaterials* **2022**, *12* (22), 3985.
(9) Gao, X.; Shi, F.; Peng, F.; Shi, X.; Cheng, C.; Hou, W.; Xie, H.; Lin, X.; Wang, X. Formulation of nanopesticide with graphene oxide as the nanocarrier of pyrethroid pesticide and its application in spider mite control. *Rsc Adv.* **2021**, *11* (57), 36089−36097.
(10) Hu, P.; Zhu, L.; Zheng, F.; Lai, J.; Xu, H.; Jia, J. Graphene oxide as a pesticide carrier for enhancing fungicide activity against Magnaporthe oryzae. *New J. Chem.* **2021**, *45* (5), 2649−2658.
(11) Guerrero Ramírez, J. R.; Ibarra Muñoz, L. A.; Balagurusamy, N.; Frías Ramírez, J. E.; Alfaro Hernández, L.; Carrillo Campos, J. Microbiology and biochemistry of pesticides biodegradation. *Int. J. Mol. Sci.* **2023**, *24* (21), 15969.
(12) Boruah, P. K.; Sharma, B.; Hussain, N.; Das, M. R. Magnetically recoverable Fe3O4/graphene nanocomposite towards efficient removal of triazine pesticides from aqueous solution: Investigation of the adsorption phenomenon and specific ion effect. *Chemosphere* **2017**, *168*, 1058−1067.
(13) Song, S.; Wan, M.; Feng, W.; Zhang, J.; Mo, H.; Jiang, X.; Shen, H.; Shen, J. Graphene oxide as the potential vector of hydrophobic pesticides: ultrahigh pesticide loading capacity and improved antipest activity. *ACS Agric. Sci. Technol.* **2021**, *1* (3), 182−191.
(14) Chen, Z.; Zhao, J.; Liu, Z.; Bai, X.; Li, W.; Guan, Z.; Zhou, M.; Zhu, H. Graphene-Delivered Insecticides against Cotton Bollworm. *Nanomaterials* **2022**, *12* (16), 2731.
(15) Liu, J.; Luo, Y.; Jiang, X.; Sun, G.; Song, S.; Yang, M.; Shen, J. Enhanced and sustained pesticidal activity of a graphene-based pesticide delivery system against the diamondback moth Plutella xylostella. *Pest Manag Sci.* **2022**, *78* (12), 5358−5365.
(16) Jayakaran, P.; Nirmala, G.; Govindarajan, L. Qualitative and Quantitative Analysis of Graphene-Based Adsorbents in Wastewater Treatment. *Int. J. Chem. Eng.* **2019**, *2019* (1), 1−17.
(17) Anegbe, B.; Ifijen, I. H.; Maliki, M.; Uwidia, I. E.; Aigbodion, A. I. Graphene oxide synthesis and applications in emerging contaminant removal: a comprehensive review. *Environ. Sci. Eur.* **2024**, *36* (1), 15.
(18) Mohan, V. B.; Lau, K.-t.; Hui, D.; Bhattacharyya, D. Graphene-based materials and their composites: A review on production, applications and product limitations. *Composites, Part B* **2018**, *142*, 200−220.
(19) Singh, R.; Samuel, M. S.; Ravikumar, M.; Ethiraj, S.; Kumar, M. Graphene materials in pollution trace detection and environmental improvement. *Environ. Res.* **2024**, *243*, 117830.
(20) Liu, B.; Zhou, P.; Liu, X.; Sun, X.; Li, H.; Lin, M. Detection of pesticides in fruits by surface-enhanced Raman spectroscopy coupled with gold nanostructures. *Food Bioprocess Technol.* **2013**, *6*, 710−718.
(21) Poudyal, D. C.; Dhamu, V. N.; Samson, M.; Muthukumar, S.; Prasad, S. Portable Pesticide Electrochem-sensor: A Label-Free Detection of Glyphosate in Human Urine. *Langmuir* **2022**, *38* (5), 1781−1790.
(22) Kilele, J. C.; Chokkareddy, R.; Redhi, G. G. Ultra-sensitive electrochemical sensor for fenitrothion pesticide residues in fruit samples using IL@ CoFe2O4NPs@ MWCNTs nanocomposite. *Microchem. J.* **2021**, *164*, 106012.
(23) Lang, T.; Xiao, M.; Cen, W. Graphene-Based Metamaterial Sensor for Pesticide Trace Detection. *Biosensors* **2023**, *13* (5), 560.
(24) Loudiki, A.; Azriouil, M.; Matrouf, M.; Laghrib, F.; Farahi, A.; Saqrane, S.; Bakasse, M.; Lahrich, S.; El Mhammedi, M. Graphene-based electrode materials used for some pesticide's detection in food samples: A review. *Inorg. Chem. Commun.* **2022**, *144*, 109891.
(25) Xue, R.; Kang, T.-F.; Lu, L.-P.; Cheng, S.-Y. Electrochemical sensor based on the graphene-nafion matrix for sensitive determination of organophosphorus pesticides. *Anal. Lett.* **2013**, *46* (1), 131−141.
(26) Kumari, K.; Singh, M. B.; Tomar, N.; Kumar, A.; Kumar, V.; Dabodhia, K. L.; Singh, P. Adsorption of pesticides using graphene oxide through computational and experimental approach. *J. Mol. Struct.* **2023**, *1291*, 136043.
(27) Wang, H.; Hu, B.; Gao, Z.; Zhang, F.; Wang, J. Emerging role of graphene oxide as sorbent for pesticides adsorption: Experimental observations analyzed by molecular modeling. *J. Mater. Sci.* **2021**, *63*, 192−202.
(28) Henna, T. K.; Pramod, K. Graphene quantum dots redefine nanobiomedicine. *Mater. Sci. Eng. C* **2020**, *110*, 110651.
(29) Singh, R. D.; Shandilya, R.; Bhargava, A.; Kumar, R.; Tiwari, R.; Chaudhury, K.; Srivastava, R. K.; Goryacheva, I. Y.; Mishra, P. K. Quantum Dot Based Nano-Biosensors for Detection of Circulating Cell Free miRNAs in Lung Carcinogenesis: From Biology to Clinical Translation. *Front. Genet.* **2018**, *9*, 616.
(30) Yan, Y.; Gong, J.; Chen, J.; Zeng, Z.; Huang, W.; Pu, K.; Liu, J.; Chen, P. Recent Advances on Graphene Quantum Dots: From Chemistry and Physics to Applications. *Adv. Mater.* **2019**, *31* (21), No. e1808283.

(31) Chong, Y.; Ma, Y.; Shen, H.; Tu, X.; Zhou, X.; Xu, J.; Dai, J.; Fan, S.; Zhang, Z. The in vitro and in vivo toxicity of graphene quantum dots. *Biomaterials* **2014**, *35* (19), 5041−5048.
(32) Fasbender, S.; Zimmermann, L.; Cadeddu, R.-P.; Luysberg, M.; Moll, B.; Janiak, C.; Heinzel, T.; Haas, R. The low toxicity of graphene quantum dots is reflected by marginal gene expression changes of primary human hematopoietic stem cells. *Sci. Rep.* **2019**, *9* (1), 12028.
(33) Jia, Q.; Yang, C.; Venton, B. J.; DuBay, K. H. Atomistic Simulations of Dopamine Diffusion Dynamics on a Pristine Graphene Surface. *ChemPhysChem* **2022**, *23* (4), No. e202100783.
(34) You, X.; He, M.; Cao, X.; Wang, P.; Wang, J.; Li, L. Molecular dynamics simulations of removal of nonylphenol pollutants by graphene oxide: Experimental study and modelling. *Appl. Surf. Sci.* **2019**, *475*, 621−626.
(35) Xie, Y.; Zhao, J.; Li, X.; Sun, J.; Yang, H. Effects of Cyfluthrin Exposure on Neurobehaviour, Hippocampal Tissue and Synaptic Plasticity in Wistar Rats. *Toxics* **2023**, *11* (12), 999.
(36) Wijewickrema, A.; Banneheke, H.; Pathmeswaran, A.; Refai, F. W.; Kauranaratne, M.; Malavige, N.; Jeewandara, C.; Ekanayake, M.; Samaraweera, D.; Thambavita, D.; et al. Efficacy and safety of oral ivermectin in the treatment of mild to moderate Covid-19 patients: a multi-centre double-blind randomized controlled clinical trial. *BMC Infectious Diseases* **2024**, *24* (1), 719.
(37) Wu, X.; Li, J.; Zhou, Z.; Lin, Z.; Pang, S.; Bhatt, P.; Mishra, S.; Chen, S. Environmental occurrence, toxicity concerns, and degradation of diazinon using a microbial system. *Front. Microbiol.* **2021**, *12*, 717286.
(38) Galadima, M.; Singh, S.; Pawar, A.; Khasnabis, S.; Dhanjal, D. S.; Anil, A. G.; Rai, P.; Ramamurthy, P. C.; Singh, J. Toxicity, microbial degradation and analytical detection of pyrethroids: A review. *Environ. Adv.* **2021**, *5*, 100105.
(39) Yang, Y.; Zhang, X.; Jiang, J.; Han, J.; Li, W.; Li, X.; Yee Leung, K. M.; Snyder, S. A.; Alvarez, P. J. Which micropollutants in water environments deserve more attention globally? *Environ. Sci. Technol.* **2022**, *56* (1), 13−29.
(40) Boukhvalov, D. W.; Katsnelson, M. I. Modeling of Graphite Oxide. *J. Am. Chem. Soc.* **2008**, *130* (32), 10697−10701.
(41) Garcia, N. A.; Awuah, J. B.; Zhao, C.; Vuković, F.; Walsh, T. R. Simulation-ready graphene oxide structures with hierarchical complexity: a modular tiling strategy. *2D Materials* **2023**, *10* (2), 025007.
(42) *Gaussian 16*; Gaussian, Inc.,: Wallingford CT, 2016 GaussView 5.0. Wallingford, E.U.A., 2016. (accessed).
(43) *Amber 2020*; University of California: San Francisco, 2020. (accessed).
(44) *Dassault Systèmes*; Dassault Systèmes, San Diego: 2021. (accessed).
(45) Sousa da Silva, A. W.; Vranken, W. F. ACPYPE - AnteChamber PYthon Parser interfacE. *BMC Research Notes* **2012**, *5* (1), 367.
(46) *GROMACS 2022 Source code*; Zenodo: 2022. (accessed).
(47) Darden, T.; York, D.; Pedersen, L. Particle mesh Ewald: An N·log(N) method for Ewald sums in large systems. *J. Chem. Phys.* **1993**, *98* (12), 10089−10092.
(48) Hess, B.; Bekker, H.; Berendsen, H. J. C.; Fraaije, J. G. E. M. LINCS: A linear constraint solver for molecular simulations. *J. Comput. Chem.* **1997**, *18*, 1463−1472.
(49) Bussi, G.; Donadio, D.; Parrinello, M. Canonical sampling through velocity rescaling. *J. Chem. Phys.* **2007**, *126* (1), 014101.
(50) Humphrey, W.; Dalke, A.; Schulten, K. VMD: Visual molecular dynamics. *J. Mol. Graphics* **1996**, *14* (1), 33−38.
(51) Valdés-Tresanco, M. S.; Valdés-Tresanco, M. E.; Valiente, P. A.; Moreno, E. gmx_MMPBSA: a new tool to perform end-state free energy calculations with GROMACS. *J. Chem. Theory Comput.* **2021**, *17* (10), 6281−6291.
(52) Moriggi, F.; Barbera, V.; Galimberti, M.; Raffaini, G. Adsorption Affinities of Small Volatile Organic Molecules on Graphene Surfaces for Novel Nanofiller Design: A DFT Study. *Molecules* **2023**, *28* (22), 7633.
(53) Subasinghege Don, V.; Kim, L.; David, R.; Nauman, J. A.; Kumar, R. Adsorption Studies at the Graphene Oxide−Liquid Interface: A Molecular Dynamics Study. *J. Phys. Chem. C* **2023**, *127* (12), 5920−5930.
(54) Alonso, M.; Woller, T.; Martin-Martinez, F. J.; Contreras-Garcia, J.; Geerlings, P.; De Proft, F. Understanding the fundamental role of pi/pi, sigma/sigma, and sigma/pi dispersion interactions in shaping carbon-based materials. *Chemistry* **2014**, *20* (17), 4931−4941.
(55) Bolibok, P.; Koter, S.; Kaczmarek-Kędziera, A.; Kowalczyk, P.; Łukomska, B.; Łukomska, O.; Boncel, S.; Wiśniewski, M.; Kaneko, K.; Terzyk, A. P. Liquid phase adsorption induced nanosizing of graphene oxide. *Carbon* **2021**, *183*, 948−957.
(56) Molla, A.; Li, Y.; Mandal, B.; Kang, S. G.; Hur, S. H.; Chung, J. S. Selective adsorption of organic dyes on graphene oxide: Theoretical and experimental analysis. *Appl. Surf. Sci.* **2019**, *464*, 170−177.
(57) Janiak, C. A critical account on $\pi-\pi$ stacking in metal complexes with aromatic nitrogen-containing ligands. *J. Chem. Soc., Dalton Trans.* **2000**, No. 21, 3885−3896.
(58) S. Araújo, W.; Caldeira Rêgo, C. R.; Guedes-Sobrinho, D.; Cavalheiro Dias, A.; Rodrigues do Couto, I.; Bordin, J. R.; Ferreira de Matos, C.; Piotrowski, M. J. Quantum Simulations and Experimental Insights into Glyphosate Adsorption Using Graphene-Based Nanomaterials. *ACS Appl. Mater. Interfaces* **2024**, 31500.
(59) Zeng, J.; Zhang, Y.; Chen, Y.; Han, Z.; Chen, X.; Peng, Y.; Chen, L.; Chen, S. Molecular dynamics simulation of the adsorption properties of graphene oxide/graphene composite for alkali metal ions. *Journal of Molecular Graphics and Modelling* **2022**, *114*, 108184.
(60) Wang, X.; Xie, H.; Wang, Z.; He, K. Graphene oxide as a pesticide delivery vector for enhancing acaricidal activity against spider mites. *Colloids Surf., B* **2019**, *173*, 632−638.
(61) Yadav, S.; Singh Raman, A. P.; Meena, H.; Goswami, A. G.; Bhawna; Kumar, V.; Jain, P.; Kumar, G.; Sagar, M.; Rana, D. K.; et al. An update on graphene oxide: applications and toxicity. *ACS omega* **2022**, *7* (40), 35387−35445.
(62) Jiang, T.; Amadei, C. A.; Lin, Y.; Gou, N.; Rahman, S. M.; Lan, J.; Vecitis, C. D.; Gu, A. Z. Dependence of Graphene Oxide (GO) Toxicity on Oxidation Level, Elemental Composition, and Size. *Int. J. Mol. Sci.* **2021**, *22* (19), 10578.

https://doi.org/10.1021/acsomega.4c06036
ACS Omega 2025, 10, 8951−8959